PERGAMON

International Journal of Heat and Mass Transfer 45 (2002) 3033–3043

International Journal of HEAT and MASS TRANSFER

www.elsevier.com/locate/ijhmt

Numerical investigation of heat transfer from a heated oscillating cylinder in a cross flow

Wu-Shung Fu *, Bao-Hong Tong

Department of Mechanical Engineering, National Chiao Tung University, Hsinchu 30056, Taiwan, ROC

Received 6 April 2001; received in revised form 19 November 2001

Abstract

A numerical simulation is performed to study the flow structures and heat transfer characteristics of a heated transversely oscillating cylinder in a cross flow. The variations of flow and thermal fields are classified into a class of moving boundary problems. The moving interfaces between the fluid and cylinder have been considered. An arbitrary Lagrangian–Eulerian kinematic description method is adopted to describe the flow and thermal fields. A penalty consistent finite element formulation is applied to solve the governing equations. The subsequent developments of the vortex shedding and heat transfer characteristics around the heated cylinder are presented in detail. The effects of Reynolds number, oscillating amplitude, oscillating speed on the flow structures and heat transfer characteristics are examined. The results show that the interaction between the oscillating cylinder and vortex shedding from the cylinder dominates the state of the wake. The flow and thermal fields may approach a periodic state in lock-in regime. The heat transfer of the cylinder in the lock-in regime is enhanced remarkably. © 2002 Published by Elsevier Science Ltd.

Keywords: Force convection; ALE method; Oscillating cylinder

1. Introduction

A phenomenon of vortex shedding induced by a flow passing through a cylinder is important in engineering applications such as heat exchangers, nuclear reactor fuel rod, and steel cable of suspension bridge. Doubtless, the heat transfer mechanism of the cylinder in the flow of vortex shedding is also interesting and important in many engineer applications.

For a flow passing through a stationary cylinder, experimental observation and numerical predictions had shown that the alternating vortex sheet in the wake of a cylinder induced lift and drag forces on the cylinder and flow to be unsteady. The unsteady flow of vortex shedding from the cylinder also caused the heat transfer on the circular cylinder to be unsteady, and the maximum local heat transfer rate was found near the front stagnation point [1–6]. Besides, Varaprasad Patnail et al. [7] adopted Galerkin weighted residual formulation to simulate a flow passing over an isolated cylinder. The effects of aiding and opposing buoyancy forces on the flow and thermal fields had been studied, and the mechanisms of vortex shedding were investigated in detail.

As for a flow passing an oscillating cylinder, there were many numerical and experimental studies [8–12] to investigate this subject. The phenomena indicated that the significant vibration happened in the vortex flow structure and the average drag force increased in the lock-in frequency. However, the studies of dealing with heat transfer problems of this subject are relatively scarce. Sreenivasan and Ramachandran [13] studied the effect of vibration on heat transfer of a horizontal cylinder normal to air stream by an experimental method and no appreciable change in the heat transfer coefficient was observed with the maximum velocity amplitude of 0.2. Saxena and Laird [14] considered a cylinder transversely oscillating in an open water channel for a flow at $Re = 3500$ and observed the increment of heat transfer to be about 60%. Leung et al. [15], Cheng et al.

* Corresponding author. Tel.: +886-3-572-7925; fax: +886-3-572-0634.

E-mail address: wsfu@cc.nctu.edu.tw (W.-S. Fu).

0017-9310/02/$ - see front matter © 2002 Published by Elsevier Science Ltd.
PII: S0017-9310(02)00016-9

Nomenclature

d	diameter of the cylinder (m)
f_c	oscillating frequency of the cylinder (s^{-1})
F_c	dimensionless oscillating frequency of the cylinder ($F_c = fd/u_c$)
h	dimensional height of the channel (m)
h_1	distance from the wall of the channel to the center of the cylinder (m)
l_c	oscillating amplitude of the cylinder (m)
L_c	dimensionless oscillating amplitude of the cylinder ($L_c = l_c/d$)
$\overline{Nu}$	average Nusselt number around the cylinder
$\overline{\overline{Nu}}$	time-averaged Nusselt number
Nu_θ	local Nusselt number
p	dimensional pressure ($N\ m^{-2}$)
p_∞	reference pressure ($N\ m^{-2}$)
P	dimensionless pressure ($P = (p - p_\infty)/\rho u_0^2$)
Pr	Prandtl number ($Pr = \upsilon/\alpha$)
r	radius of the cylinder (m)
R	dimensionless radius ($R = r/d$)
Re	Reynolds number ($Re = u_0 d/\upsilon$)
t	dimensional time (s)
T	dimensional temperature (K)
T_c	dimensional temperature of the cylinder (K)
T_0	dimensional temperature of the inlet fluid (K)
u, v	dimensional velocities in x and y directions ($m\ s^{-1}$)
U, V	dimensionless velocities in X and Y directions ($U = u/u_0, V = v/u_0$)
u_0	dimensional velocities of the inlet fluid ($m\ s^{-1}$)
v_c	dimensional oscillating velocity of the cylinder ($m\ s^{-1}$)
V_c	dimensionless oscillating velocity of the cylinder ($V_c = v_c/u_0$)
v_m	dimensional maximum oscillating velocity of the cylinder ($m\ s^{-1}$)
V_m	dimensionless maximum oscillating velocity of the cylinder ($V_m = v_m/u_0$)
$\hat{v}$	dimensional mesh velocity in y-direction ($m\ s^{-1}$)
$\hat{V}$	dimensionless mesh velocity in Y-direction ($\hat{V} = \hat{v}/u_0$)
w	dimensional length of the channel
w_1	dimensional distance from the inlet of the channel to the cylinder
w_2	dimensional distance from the outlet of the channel to the cylinder
x, y	dimensional Cartesian coordinates (m)
X, Y	dimensionless Cartesian coordinates ($X = x/d, Y = y/d$)

Greek symbols

α	thermal diffusivity ($m^2\ s^{-1}$)
Φ	computational variables
λ	penalty parameter
υ	kinematic viscosity ($m^2\ s^{-1}$)
π	ratio of the circumference of a circle to its diameter
θ	dimensionless temperature ($\theta = (T - T_0)/(T_c - T_0)$)
ρ	density ($kg\ m^{-3}$)
τ	dimensionless time ($\tau = tu_0/d$)
τ_p	dimensionless time of one oscillating cycle
Ψ	dimensionless stream function

Others

$\|\|$	absolute value

[16], and Gau et al. [17] experimentally investigated heat transfer around a heated oscillating circular cylinder. The results found that the enhancement of heat transfer was proportional to the magnitude of oscillating frequency and amplitude of the circular cylinder. Due to the difficulty of numerical computation, there were a few papers to study the above problem numerically. Karanth et al. [18] studied the flow over a transversely oscillating cylinder in infinite domain at $Re = 200$ numerically. In order to simplify the computation, the non-inertial reference frame adopted for computing this subject and the result showed that the heat transfer rate of the oscillating cylinder increased with the increasing of velocity. Cheng et al. [19] adopted the same numerical method to study the effect of transverse oscillation on the flow patterns and heat transfer from a cylinder. The results indicated that the heat transfer increased remarkably as the flow approached the lock-in regime, in which the cylinder oscillating frequency is near the natural vortex shedding frequency; however, outside the lock-in regime the heat transfer was almost unaffected by the oscillation of the cylinder. Most studies mentioned above focused on free surface boundary. The study of flow of vortex shedding and heat transfer of circular cylinder in a channel is seldom investigated.

The subject of the present work is therefore to investigate the variations of flow and thermal fields of the flow passing over a heated transversely oscillating cylinder in a channel. Due to the interaction between the flow and oscillating cylinder, the variations of the flow and thermal fields become time-dependent and belong to a class of the moving boundary problem. In the past, a structure oscillating or moving in a flowing fluid was conveniently regarded as a stationary one in the flow or

a non-inertial reference frame moving with the structure for analyzing the above problem. Those methods are used to solve the problem of free surface boundary; nevertheless, those seldom solve the problem with the fixed boundary. However, due to the continuity of flow, the fluid near the structure will simultaneously replenish the blank space induced by the movement of the structure. For simulating the problem more realistically, the interfaces between the fluid and cylinder under moving situation have been taken into consideration, and this problem is then hardly analyzed by either the Lagrangian or the Eulerian kinematic description methods solely. An arbitrary Lagrangian–Eulerian (ALE) kinematic description method [20], which combines the characteristics of the Lagrangian and Eulerian kinematic description method, is an appropriate kinematic description method to describe this problem. In the ALE method, the computational meshes may move with the fluid (Lagrangian), be held fixed (Eulerian), or be moved in prescribed way. The detail of the kinematic theory of the ALE method is delineated in Hughes et al. [21], Donea et al. [22], and Ramaswamy [23].

Consequently, the ALE method is adopted to investigate numerically the variations of the flow and thermal fields induced by the transversely heated oscillating cylinder in a cross flow. Thus, it could simulate this problem more realistically in this study. A consistent penalty finite element method is applied to solve the governing equations. The subsequent development of the vortex shedding and the heat transfer characteristics around the heated cylinder are presented in detail. The effects of Reynolds number, oscillating speed, and oscillating frequency of the cylinder on the flow structures and heat transfer characteristics are investigated.

2. Physical model

The physical model used in this study is shown in Fig. 1. A two-dimensional channel with height h and length w is used to simulate this problem. An isothermal cylinder of diameter d with constant temperature T_c is set within the channel. The distances from the inlet and outlet of the channel to the cylinder are w_1 and w_2, respectively. The inlet velocity u_0 and temperature T_0 of the fluid are uniform. Initially, the cylinder is stationary at the position of the center of the channel and the fluid flows steadily. The distance from the wall of the channel to the center of the cylinder is h_1. As the time $t > 0$, the cylinder is in oscillating motion normal to the inlet flow with velocity $v_c = v_m \cos(2\pi f_c t)$. The blockage ratio (d/h) is 0.1. The behavior of the oscillating cylinder and the flow then affects mutually, and the variations of the flow field become time-dependent and are classified into a class of moving boundary problems. As a result, the ALE method is properly utilized to analyze this problem.

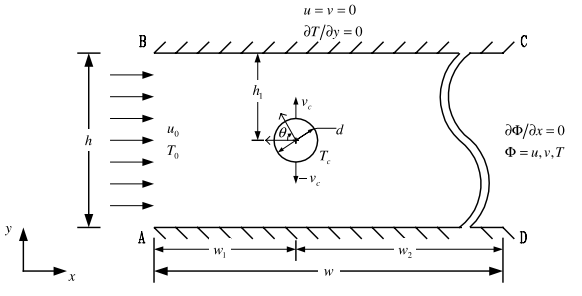

Fig. 1. Physical model.

For facilitating the analysis, the following assumptions are made.

(1) The fluid is air and the flow field is two-dimensional, incompressible and laminar.
(2) The fluid properties are constant and the effect of the gravity is neglected.
(3) The no-slip condition is held on the interfaces between the fluid and cylinder.

Based upon the characteristics scales of d, u_0, ρu_0^2 and T_0, the dimensionless variables are defined as follows:

$$X = \frac{x}{d}, \quad Y = \frac{y}{d}, \quad U = \frac{u}{u_0}, \quad V = \frac{v}{u_0}, \quad \hat{V} = \frac{\hat{v}}{u_0},$$
$$V_c = \frac{v_c}{u_0}, \quad V_m = \frac{v_m}{u_0}, \quad F_c = \frac{f_c d}{u_0}, \quad P = \frac{p - p_\infty}{\rho u_0^2},$$
$$\tau = \frac{t u_0}{d}, \quad \theta = \frac{T - T_0}{T_c - T_0}, \quad Re = \frac{u_0 d}{\upsilon}, \quad Pr = \frac{\upsilon}{\alpha}, \tag{1}$$

where $\hat{v}$ is the mesh velocity, v_c, f_c and v_m are the oscillating velocity, the oscillating frequency of the cylinder, and the maximum oscillating velocity of the cylinder, respectively.

According to the above assumptions and dimensionless variables, the dimensionless ALE governing equations [22–25] are expressed as the following equations:

Continuity equation

$$\frac{\partial U}{\partial X} + \frac{\partial V}{\partial Y} = 0. \tag{2}$$

Momentum equation

$$\frac{\partial U}{\partial \tau} + U\frac{\partial U}{\partial X} + \left(V - \hat{V}\right)\frac{\partial U}{\partial Y} = -\frac{\partial P}{\partial X} + \frac{1}{Re}\left(\frac{\partial^2 U}{\partial X^2} + \frac{\partial^2 U}{\partial Y^2}\right), \tag{3}$$

$$\frac{\partial V}{\partial \tau} + U\frac{\partial V}{\partial X} + \left(V - \hat{V}\right)\frac{\partial V}{\partial Y} = -\frac{\partial P}{\partial Y} + \frac{1}{Re}\left(\frac{\partial^2 V}{\partial X^2} + \frac{\partial^2 V}{\partial Y^2}\right). \tag{4}$$

Energy equation

$$\frac{\partial\theta}{\partial\tau}+U\frac{\partial\theta}{\partial X}+\left(V-\hat{V}\right)\frac{\partial\theta}{\partial Y}=\frac{1}{RePr}\left(\frac{\partial^2\theta}{\partial X^2}+\frac{\partial^2\theta}{\partial Y^2}\right). \quad (5)$$

As the time $\tau > 0$, the boundary conditions are as follows:

On the inlet surface AB

$$U=1, \quad V=0, \quad \theta=0. \quad (6)$$

On the wall BC and AD

$$U=0, \quad V=0, \quad \frac{\partial\theta}{\partial Y}=0. \quad (7)$$

On the outlet surface CD

$$\frac{\partial U}{\partial X}=0, \quad \frac{\partial V}{\partial X}=0, \quad \frac{\partial\theta}{\partial X}=0. \quad (8)$$

On the interfaces between the fluid and cylinder

$$U=0, \quad V=V_c, \quad \theta=1. \quad (9)$$

3. Numerical method

The governing equations and boundary conditions are solved through the Galerkin finite element formulation and a backward scheme is adopted to deal with the time terms of the governing equations. The pressure is eliminated from the governing equations using the consistent penalty method [26]. The velocity and temperature terms are expressed as quadrilateral element and eight-node quadratic Lagrangian interpolation function. The Newton–Raphson iteration algorithm is utilized to simplify the non-linear terms in the momentum equations. The discretion processes of the governing equations are similar to the one used in Fu et al. [27]. Then, the momentum equations (3) and (4) can be expressed as the following matrix form:

$$\sum_1^{n_e}\left([A]^{(e)}+[K]^{(e)}+\lambda[L]^{(e)}\right)\{q\}^{(e)}_{\tau+\Delta\tau}=\sum_1^{n_e}\{f\}^{(e)}, \quad (10)$$

where

$$\left(\{q\}^{(e)}_{\tau+\Delta\tau}\right)^{\mathrm{T}}=\langle U_1,U_2,\ldots,U_8,V_1,V_2,\ldots,V_8\rangle^{m+1}_{\tau+\Delta\tau}, \quad (11)$$

$[A]^{(e)}$ includes the (m)th iteration values of U and V at time $\tau+\Delta\tau$; $[K]^{(e)}$ includes the shape function, $\hat{V}$, and time differential terms; $[L]^{(e)}$ includes the plenty function; $[f]^{(e)}$ includes the known values of U and V at time τ and (m)th iteration values of U and V at time $\tau+\Delta\tau$.

The energy equation (5) can be expressed as the following matrix form:

$$\sum_1^{n_e}\left([M]^{(e)}+[Z]^{(e)}\right)\{c\}^{(e)}_{\tau+\Delta\tau}=\sum_1^{n_e}\{r\}^{(e)}, \quad (12)$$

where

$$\left(\{c\}^{(e)}_{\tau+\Delta\tau}\right)^{\mathrm{T}}=\langle\theta_1,\theta_2,\ldots,\theta_8\rangle_{\tau+\Delta\tau}, \quad (13)$$

$[M]^{(e)}$ includes the values of U and V at time $\tau+\Delta\tau$; $[Z]^{(e)}$ includes the shape function, $\hat{V}$, and time differential terms; $[r]^{(e)}$ includes the known values of θ at time τ.

In Eqs. (10) and (12), Gaussian quadrature procedure are conveniently used to execute the numerical integration. The terms with the penalty parameter λ are integrated by 2×2 Gaussian quadrature, and the other terms are integrated by 3×3 Gaussian quadrature. The value of penalty parameter λ used in this study is 10^6. The frontal method solver is applied to solve Eqs. (10) and (12). The mesh velocity $\hat{V}$ is linearly distributed and inversely proportional to the distance between the nodes of the computational elements and cylinder.

A brief outline of the solution procedures are described as follows:

(1) Determine the optimal mesh distribution and number of the elements and nodes.
(2) Solve the values of the U, V and θ at the steady state and regard them as the initial values.
(3) Determine the time step $\Delta\tau$ and the mesh velocity $\hat{V}$ of the computational meshes.
(4) Update the coordinates of the nodes and examine the determinant of the Jacobian transformation matrix to ensure the one to one mapping to be satisfied during the Gaussian quadrature numerical integration.
(5) Solve Eq. (10), until the following criteria for convergence are satisfied:

$$\left|\frac{\Phi^{m+1}-\Phi^m}{\Phi^{m+1}}\right|_{\tau+\Delta\tau}<10^{-3}, \quad (14)$$

where $\Phi = U$ and V,

and substitute the U and V into Eq. (12) to obtain θ.
(6) Continue the next time step calculation until periodic solutions are attained.

4. Results and discussion

The working fluid is air with $Pr = 0.71$. The main parameters of Reynolds number Re, maximum oscillating velocity V_m, and oscillating frequency F_c are examined and the combinations of these parameters are tabulated in Table 1.

The local Nusselt number is calculated by the following equation

$$Nu_\theta=-\left.\frac{\partial\theta}{\partial R}\right|_{R=1/2}. \quad (15)$$

Table 1
Computed parameter combinations

	Re	V_m	F_c	L_c
Case 1	200	0.5	0.1	0.8
Case 2	200	0.5	0.2	0.4
Case 3	200	0.5	0.4	0.2
Case 4	200	0.25	0.2	0.2
Case 5	200	1	0.2	0.8
Case 6	100	1	0.2	0.8
Case 7	500	1	0.2	0.8

The average Nusselt number around the cylinder is expressed as follows.

$$Nu = \frac{1}{2\pi}\int_0^{2\pi} Nu_\theta \,\mathrm{d}\theta. \tag{16}$$

The time-averaged Nusselt number per cycle is defined by

$$\overline{Nu} = -\frac{1}{\tau_p}\int_0^{\tau_p} Nu \,\mathrm{d}\tau. \tag{17}$$

For matching the boundary conditions at the inlet and outlet of the channel mentioned above, the lengths from the inlet and outlet to the cylinder are determined by numerical tests and equal to 10.0 and 30.0, respectively. To obtain an optimal computational mesh, three different non-uniform distributed elements, which provide a finer element resolution near the cylinder and walls, are used for the mesh tests. Fig. 2 shows the velocity and temperature profiles along the line through the center of the cylinder and parallel the Y-axis at the steady state under $Re = 500$. Based upon the results, the computational mesh with 4524 elements, which is corresponding to 13 960 nodes, is used for all cases in this study.

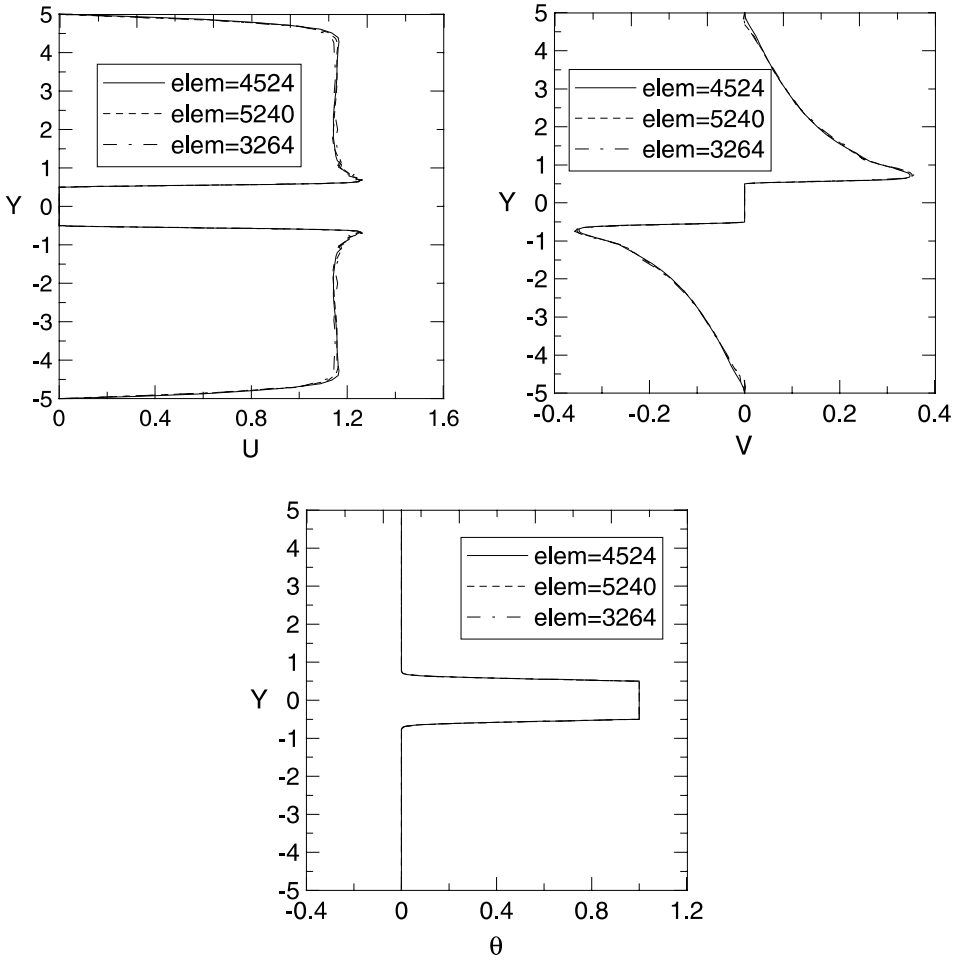

Fig. 2. Comparison of the velocity and temperature profiles along the line through the center of the cylinder and parallel the Y-axis for different mesh.

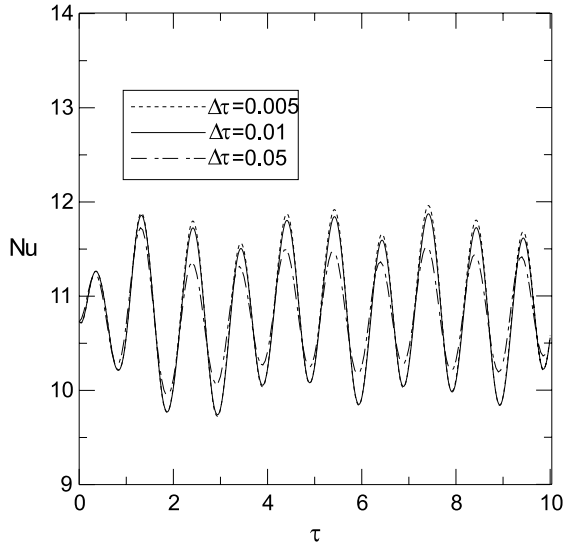

Fig. 3. Comparison of the variations of the average Nusselt numbers around the cylinder for different time steps $\Delta\tau$.

In addition, an implicit scheme is employed to deal with the time differential terms of the governing equations. Three different time steps $\Delta\tau = 0.05$, 0.01, and 0.005 at $Re = 500$, $V_m = 1$, and $F_c = 0.5$, are executed for the time step tests. The variations of the average Nusselt number around the cylinder Nu with time are shown in Fig. 3, and the time step $\Delta\tau = 0.01$ is chosen for all cases in this study.

The dimensionless stream function Ψ is defined as

$$U = \frac{\partial \Psi}{\partial Y}, \quad V = -\frac{\partial \Psi}{\partial X}. \tag{18}$$

For clearly indicating the variations of the flow and thermal fields, the streamlines and isothermal lines in the vicinity of the cylinder are presented only. Besides, the sign "arrow" in the subsequent figures is to indicate the moving direction of the cylinder.

Fig. 4(a) shows the comparison of the distributions of local Nusselt number on a stationary cylinder of the present study with existing studies [2,5,7]. The maximum local heat transfer rate is found at the upstream stagnation point. The consistence between the present study and other studies is available. Fig. 4(b), the average Nusselt numbers of the present study at steady state for different Reynolds numbers are compared with the previous studies [1,16]. The deviation among the results is small.

Fig. 5 shows the transient developments of the streamlines for case 2. At the time $\tau = 0$, the cylinder is stationary and the flow is steady. The formation of large recirculation zones is observed behind the cylinder, as shown in Fig. 5(a). As time $\tau > 0$, the cylinder starts to oscillate with the oscillating velocity $V_c = V_m \cos(2\pi F_c \tau)$ and oscillating frequency $F_c = 0.2$. As shown in Fig. 5(b), the cylinder moves upward. The fluid near the top region of the cylinder is pressed by the surface of cylinder. Conversely, the fluid near the bottom region of the cylinder simultaneously replenishes the vacant space induced by the movement of the cylinder due to the continuity of the flow. The cylinder turns downward as it reaches the maximum upper amplitude. As shown in Fig. 5(c), the cylinder is on the way to move downward. Since the moving direction of the cylinder is changed, the fluid near the top region of the cylinder replenishes the vacant space similar to the phenomenon mentioned above, and causes a new recirculation zone to form around the rear of the cylinder. Afterward, the fluid near the bottom region of the cylinder is continuously pressed by the cylinder. As a result, the recirculation zone around the rear of the cylinder is shed from the cylinder, and the vortex shedding begins to happen, as shown in

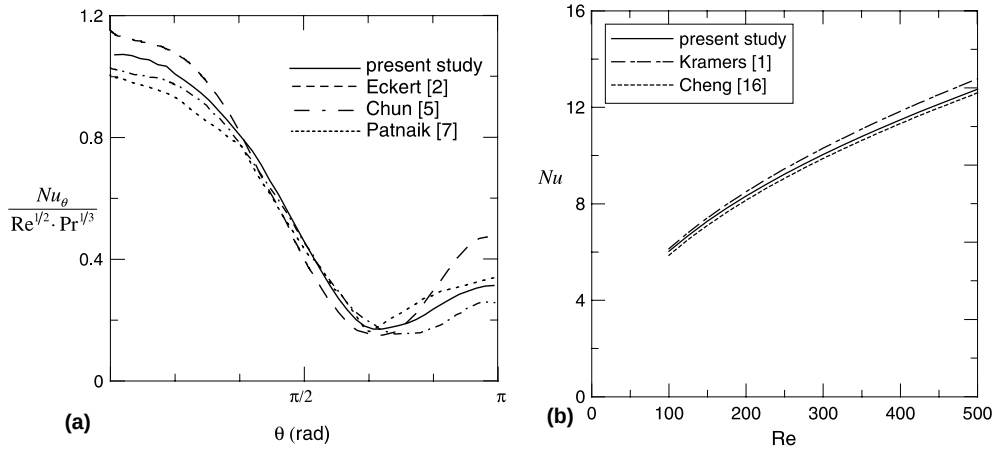

Fig. 4. Comparison of Nusselt numbers with existing studies: (a) local Nusselt number; (b) average Nusselt numbers.

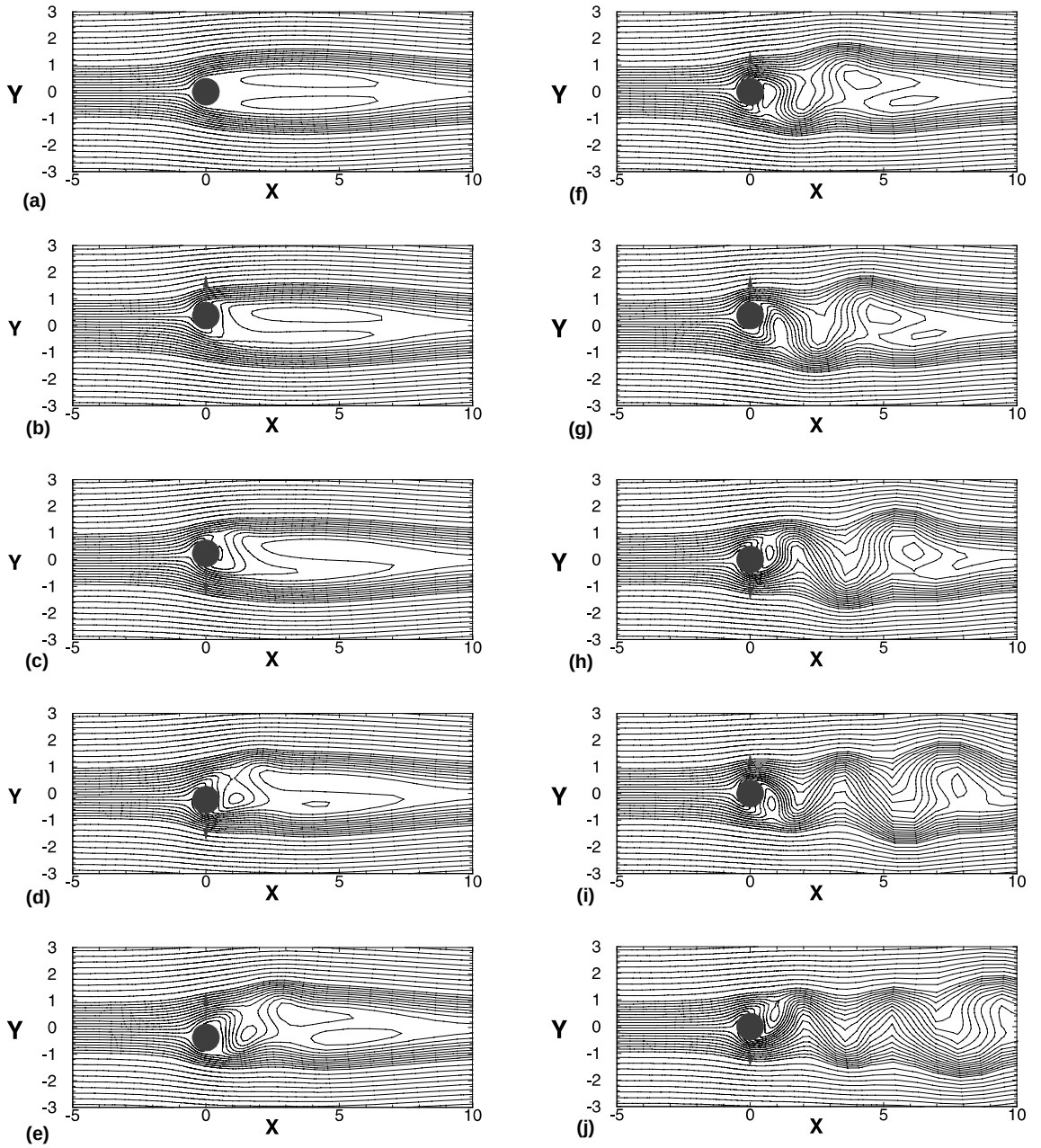

Fig. 5. The transient developments of streamlines for case 2: (a) $\tau = 0$; (b) $\tau = 1$; (c) $\tau = 2$; (d) $\tau = 3$; (e) $\tau = 4$; (f) $\tau = 5$; (g) $\tau = 6$; (h) $\tau = 7.5$; (i) $\tau = 10$; (j) $\tau = 12.5$.

Fig. 5(d). As the cylinder reaches the maximum downward amplitude, the cylinder returns upward immediately shown in Figs. 5(e)–(g). The new recirculation zone is formed around the rear of the cylinder and shed from the cylinder. Due to the vortex shedding and the oscillating motion of the cylinder, the large recirculation zones behind the cylinder are difficult to maintain their original situations, which causes the large recirculation zones to be split into small vortices and to flow to the downstream. As the time increases, since the cylinder is in oscillating motion, the formation of the recirculation zones around the rear region of the cylinder becomes periodic. Besides, due to the drastic swing of the cylinder, the vortices are scattered in the flow gradually. Finally, the flow becomes wavy motion, as shown in Figs. 5(h)–(j). The behaviors of the oscillating

cylinder and shedding vortex dominate the state of the wake.

Figs. 6(a)–(e) show the variations of the streamlines and isothermal lines for case 2 during one periodic cycle. The streamlines and isothermal lines at the time $\tau = 55$ (Fig. 6(a)) are identical with those at the time $\tau = 60$ (Fig. 6(e)), which means that the variations of the flow and thermal fields become a periodic motion with time.

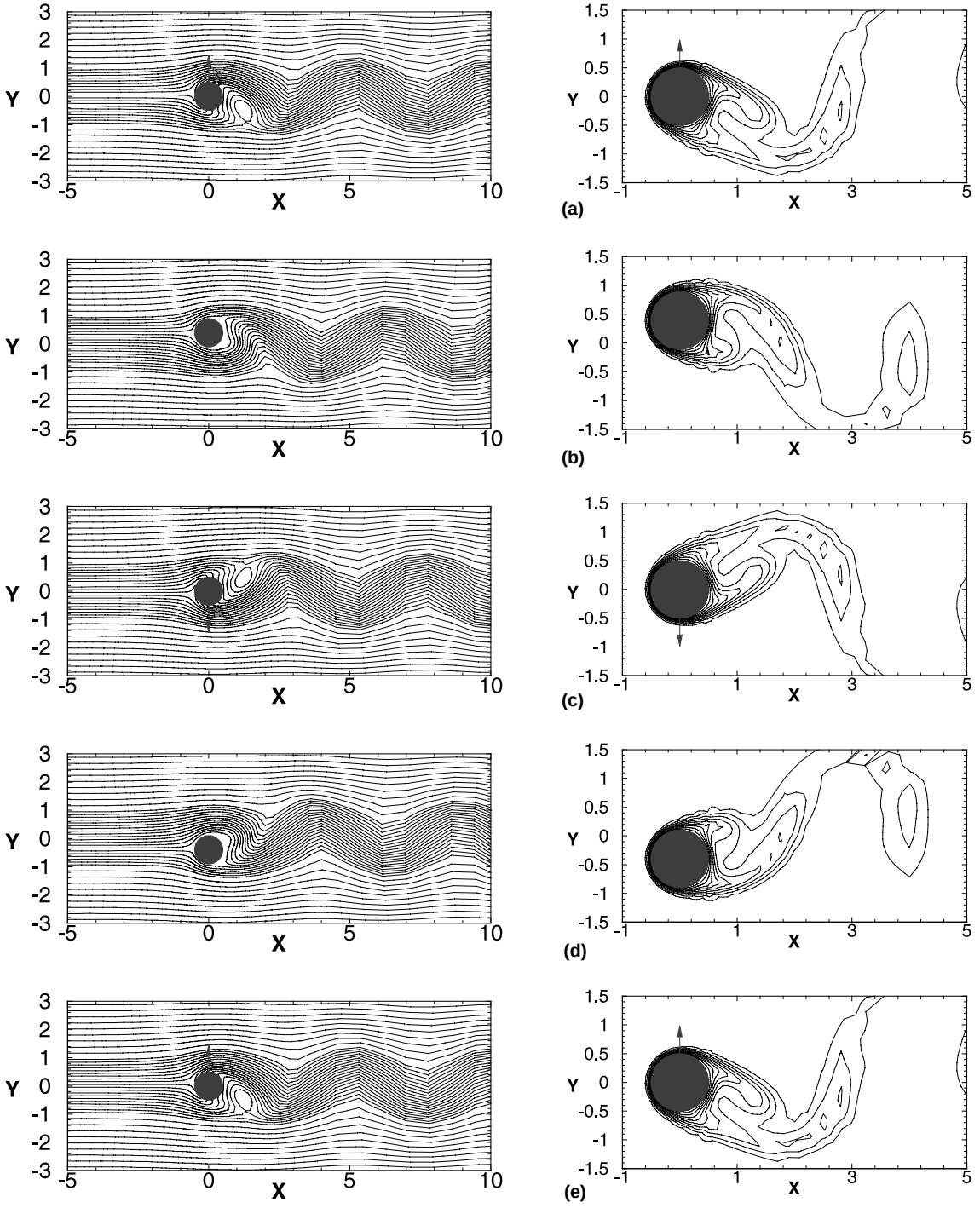

Fig. 6. The variations of the streamlines and isothermal lines during one periodic cycle under $Re = 200$, $V_m = 0.5$, and $F_c = 0.2$ situation.

The distributions of local Nusselt number on the stationary cylinder and oscillating cylinder in one periodic cycle are shown in Fig. 7. The maximum heat transfer coefficient approximately occurs at the front stagnation point, and the minimum heat transfer coefficient occurs at the near separation point position. At the stage of quarter cycle ($\tau_p/4$), the cylinder stops at the highest amplitude, as shown in Fig. 6(b). Since the flow behind the cylinder becomes wavy motion, the disturbance of flow field behind the cylinder is increased. As a result, comparing with the stationary cylinder, the heat transfer rate on the rear region ($\pi/2 < \theta < 3\pi/2$) of the oscillating cylinder is enhanced obviously. Since the fluid is pressed by the upward cylinder, the heat transfer rate on the top region of the cylinder ($\theta < \pi/2$) increases slightly relating to that of the stationary cylinder. At the stage of half cycle ($2\tau_p/4$), the cylinder moves downward with the maximum oscillation velocity, as shown in Fig. 6(c). The fluid skims over the downward cylinder, the heat transfer rate of the upper region ($\theta < \pi/2$) of the cylinder is then smaller than that of the stationary cylinder, and the position of the minimum heat transfer rate on the top surface of the cylinder moves forward slightly. The fluid near the lower region ($\pi/2 < \theta < \pi$) is pressed by the cylinder, therefore the heat transfer rate in this region is apparently larger than that of the stationary cylinder, and the position of minimum heat transfer on the bottom surface of the cylinder moves backward. Afterward, at the stage of three-fourths periodicity ($3\tau_p/4$), the cylinder stops at the lowest position, as shown in Fig. 6(d). Similar to the phenomena of the stage of quarter cycle ($\tau_p/4$), the heat transfer rate on the rear region of the oscillating cylinder is enhanced obviously. Oppositely, because of the different moving directions of the cylinder at the stages of $\tau_p/4$ and $3\tau_p/4$, the heat transfer rate on the bottom surface of the cylinder ($\theta > 3\pi/2$) increases slightly similar to that of the stationary cylinder, but the heat transfer rate on the top surface ($\theta < \pi/2$) is close to that of the stationary cylinder. Finally, the cylinder turns upward to finish one periodicity ($4\tau_p/4$), as shown Fig. 6(e). The cylinder moves upward with the maximum velocity, opposite to the phenomena of downward movement of the cylinder, the heat transfer rate on the upper region ($0 < \theta < \pi$) of the cylinder increases substantially, but the heat transfer rate on the lower region ($3\pi/2 < \theta < 2\pi$) of the oscillating cylinder is slightly lower than that of the stationary cylinder.

When the oscillating frequency approaches the natural shedding frequency, it would cause the lock-in phenomenon to happen [8–12]. For a flow passing through a stationary cylinder, the natural frequency of vortex shedding is about 0.2 over a range of Reynolds number from 2×10^2 to 10^4. Fig. 8 shows the variations of average Nusselt number Nu of the cylinder with time for different oscillating frequencies under $Re = 200$ and $V_m = 0.5$, situation. Comparing with the stationary cylinder, the heat transfer rates of the oscillating cylinder are increased about 10%, 13%, and 8% relating to the stationary one for oscillating frequencies of $F_c = 0.1$ (case 1), $F_c = 0.2$ (case 2), and $F_c = 0.4$ (case 3), respectively. It can be observed that as the oscillating frequency is in the lock-in regime ($F_c = 0.2$), the heat transfer rate is enhanced apparently, and the flow

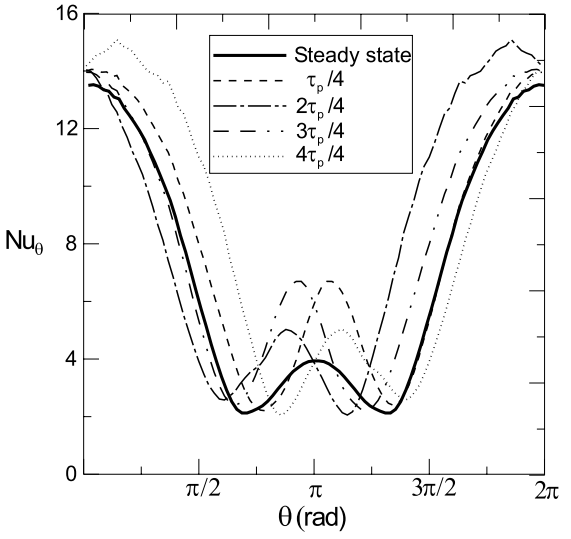

Fig. 7. The distributions of local Nusselt number on the oscillating cylinder for case 2.

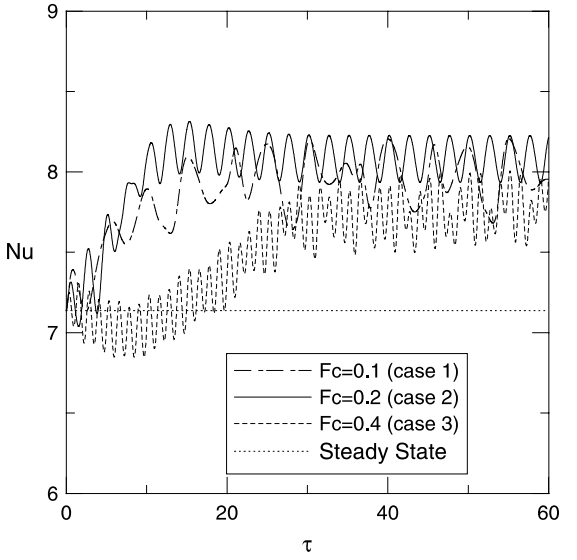

Fig. 8. The variations of average Nusselt number around the cylinder with time for different oscillating frequencies under $Re = 200$ and $V_m = 0.5$ situation.

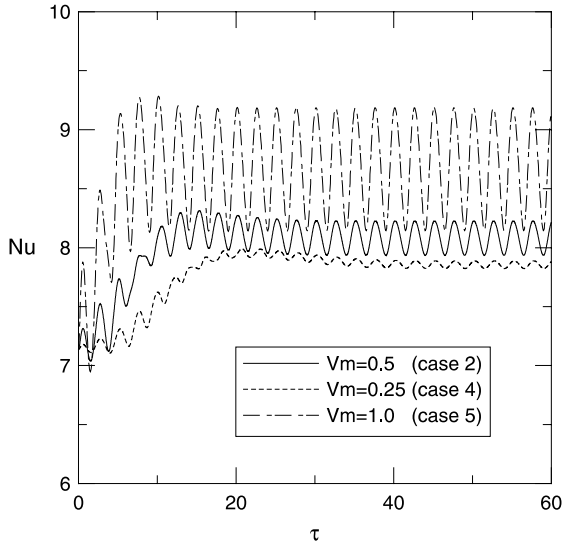

Fig. 9. The variations of average Nusselt number around the cylinder with time for different oscillating velocities under $Re = 200$ and $F_c = 0.2$ situation.

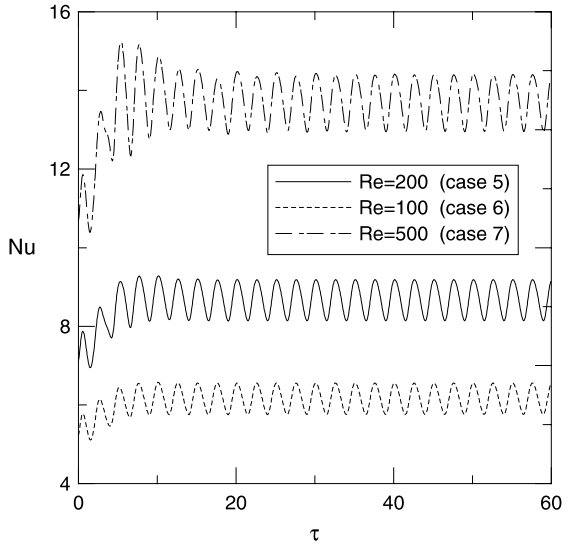

Fig. 10. The variations of average Nusselt number around the cylinder with time for various Reynolds numbers under $F_c = 0.2$ and $V_m = 0.5$ situation.

and the thermal fields approach a periodic state with time. Conversely, when the values of F_c are equal to 0.1 and 0.4, the flows become the unlock-in flow, the enhancement for the heat transfer rate of these flows are not as significant as that in the lock-in regime, and the variations of the flow and thermal fields are irregular in those frequencies. The phenomenon is consistent with the literature [16–19] for a cylinder oscillating in a flow.

The effects of the oscillating speed on the heat transfer are shown in Fig. 9 for the $Re = 200$ and $F_c = 0.2$. Comparing with the stationary cylinder, the heat transfer rates around the oscillating cylinder are increased about 10.2%, 13.3%, and 21.9% for the maximum oscillating velocity $V_m = 0.25$ (case 4), $V_m = 0.5$ (case 2), $V_m = 1.0$ (case 5), respectively. As the oscillating velocity of the cylinder increases, the variations of the flow become more drastic. Consequently, the heat transfer rate is enhanced remarkably with the increment of the oscillating velocity.

The effects of the Reynolds number on the heat transfer are shown in Fig. 10 for the $V_m = 1.0$ and $F_c = 0.2$. The heat transfer rates around the cylinder are increased about 17.8%, 21.9%, and 28.7% for the Reynolds number of 100 (case 6), 200 (case 5), and 500 (case 7), respectively. The heat transfer rate is enhanced remarkably with the increment of the Reynolds number.

5. Conclusions

The flow structures and the heat transfer characteristics of a heated transversely oscillating cylinder in a cross flow are investigated numerically. Some conclusions are summarized as follows:

1. The interaction between the oscillation cylinder and vortex shedding from the cylinder dominates the state of the wake. As the flow is in the lock-in regime, the frequency of the vortice shedding is near the oscillating frequency of the cylinder, the flow and thermal fields would approach a periodic state.
2. The heat transfer rate is enhanced remarkably as the oscillating frequency of the cylinder approaches the natural shedding frequency.
3. The heat transfer rate is increased apparently when the oscillating velocity of the cylinder and the Reynolds number are increased.
4. This study solves the moving boundary problem by ALE method and simulates the flow passing over a oscillating cylinder in a channel, successfully. Further, it could analyze the effect of the oscillating cylinder on the heated block mounted on the channel, which is interesting and important in many engineer applications.

Acknowledgements

The support of this work by the National Science Council of Taiwan, ROC, under contract NSC89-2212-E009-019 is gratefully acknowledged.

References

[1] H.A. Kramers, Heat transfer from sphere to flowing media, Physics 12 (1946) 61–80.

[2] E.R.G. Eckert, E. Soehngen, Distribution of heat transfer coefficient around circular cylinders in cross flow at Reynolds numbers from 20 to 500, J. Heat Transfer 74 (1952) 343–347.

[3] S.C.R. Dennis, J.D. Hudson, N. Smith, Steady laminar forces convection from a circular cylinder at low Reynolds numbers, Phys. Fluids 11 (5) (1968) 933–940.

[4] G.E. Karniadakis, Numerical simulation of forced convection heat transfer from a cylinder in cross flow, Int. J. Heat Mass Transfer 31 (1) (1988) 407–418.

[5] W. Chun, R.F. Boehm, Calculation of forced flow and heat transfer around a cylinder in cross flow, Numer. Heat Transfer 15 (1989) 101–122.

[6] Y.-T. Yang, C.-K. Chen, S.-R. Wu, Transient laminar forced convection from a circular cylinder using a body-fitted coordinate system, J. Thermophys. 6 (1992) 184–188.

[7] B.S. Varaprasad Patnaik, P.A. Aswatha Narayana, K.N. Seetharamu, Numerical simulation of vortex shedding past a circular cylinder under the influence of buoyancy, Int. J. Heat Mass Transfer 42 (1999) 3495–3507.

[8] Y. Tanida, A. Okaijma, Y. Watanabe, Stability of a circular cylinder oscillating in uniform flow, J. Fluid Mech. 61 (1973) 769–784.

[9] S.E. Hurlbut, M.L. Spaulding, F.M. White, Numerical solution for laminar two dimensional flow about a cyclinder oscillating in a uniform stream, J. Fluids Eng. 104 (1982) 214–222.

[10] R. Chilukuri, Incompressible laminar flow pass a transversely vibrating cylinder, J. Fluids Eng. 109 (1987) 166–171.

[11] M.O. Griffin, M.S. Hall, Review-vortex shedding lock-on and flow control in bluff body wakes, J. Fluids Eng. 113 (1991) 526–537.

[12] J. Zhang, C. Dalton, Interaction of a steady approach flow and a circular cylinder undergoing forced oscillation, J. Fluids Eng. 119 (1997) 808–813.

[13] K. Sreenivasan, A. Ramachandran, Effect of vibration on heat transfer from a horizontal cylinder to a normal air stream, Int. J. Heat Mass Transfer 3 (1961) 60–67.

[14] U.C. Saxena, A.D.K. Laird, Heat transfer from a cylinder oscillating in a cross flow, J. Heat Transfer 100 (1978) 684–689.

[15] C.T. Leung, N.W.M. Ko, K.H. Ma, Heat transfer from a vibrating cylinder, J. Sound Vib. 75 (4) (1981) 581–582.

[16] C.-H. Cheng, H.-N. Chen, W. Aung, Experimental study of the effect of transverse oscillation on convection heat transfer from a circular cylinder, J. Heat Transfer 119 (1997) 474–482.

[17] C. Gau, J.M. Wu, C.Y. Liang, Heat transfer enhancement and vortex flow structure over a heated cylinder oscillating in the cross flow direction, J. Heat Transfer 121 (1999) 789–795.

[18] D. Karanth, G.W. Rankin, K. Sridhar, Afinite difference calculation of forced convective heat transfer from an oscillating cylinder, Int. J. Heat Mass Transfer 37 (1994) 1619–1630.

[19] C.-H. Cheng, J.-L. Hong, W. Aung, Numerical prediction of lock-on effect on convective heat transfer from a transversely oscillating circular cylinder, Int. J. Heat Mass Transfer 40 (1997) 1825–1834.

[20] C.W. Hirt, A.A. Amsden, H.K. Cooks, An arbitrary Lagrangian–Eulerian computing method for all flow speeds, J. Comput. Phys. 14 (1974) 227–253.

[21] T.J.R. Hughes, W.K. Liu, T.K. Zimmermann, Lagrangian–Eulerian finite element formulation for incompressible viscous flows, Comput. Meth. Appl. Mech. Eng. 29 (1981) 329–349.

[22] J. Donea, S. Giuliani, J.P. Halleux, An arbitrary Lagrangian–Eulerian finite element method for transient dynamic fluid-structure interactions, Comput. Meth. Appl. Mech. Eng. 33 (1982) 689–723.

[23] B. Ramaswamy, Numerical simulation of unsteady viscous free surface flow, J. Comput. Phys. 90 (1990) 396–430.

[24] W.S. Fu, S.J. Yang, Numerical simulation of heat transfer induced by a body moving in the same direction as flowing fluids, Heat Mass Transfer 36 (2000) 257–264.

[25] W.S. Fu, S.J. Yang, Heat transfer induced by a body moving in opposition to a flowing fluid, Int. J. Heat Mass Transfer 44 (2001) 89–98.

[26] J.N. Reddy, D.K. Gartling, in: The Finite Element Method in Heat Transfer and Fluid Dynamics, CRC Press, Ann Arbor, 1994, pp. 47–51.

[27] W.S. Fu, T.M. Kau, W.J. Shieh, Transient laminar natural convection in an enclosure from steady state to stationary state, Numer. Heat transfer: Part A 18 (1990) 189–212.